

Site-dependent NMR Spin-lattice Relaxation in the Superconducting State of an Iron Pnictide Superconductor

L. Ma ¹, J. Zhang ², G. F. Chen ¹, T.-L. Xia ¹, J. B. He¹, D. M. Wang¹, and W. Yu ^{1*}

¹*Department of Physics, Renmin University of China,
Beijing 100872, China*

²*School of Energy and Power Engineering,
North China Electric Power University,
Beijing 102206, China*

(Dated: February 23, 2024)

In a conventional superconductor, the spin-lattice relaxation rate on all nuclei should have the same temperature dependence below T_C . We performed ^{23}Na , ^{75}As , and ^{59}Co NMR studies on single crystals of $\text{NaFe}_{0.95}\text{Co}_{0.05}\text{As}$, and found that spin-lattice relaxation rates show very different temperature dependent power-law behavior on three sites. We propose that such site-dependent behavior is due to the facts that the superconductor has two gaps of very different size. The power-law exponent of each nucleus is affected by the strength of the hyperfine coupling to the small gap. We also found that the large superconducting gap on the cobalt site is smaller than on other two sites. It suggests a local suppression of the superconducting gap on the dopant site.

PACS numbers: 74.70.-b, 76.60.-k

The Hebel-Slichter formulation is very successful in analyzing the NMR spin-lattice relaxation rate (SLRR) of superconductors^{1,2}. Below T_C , the scheme can be used to determine the symmetry and the amplitude of the superconducting gap. For example, the low-temperature SLRR usually shows a gaped behavior with a coherence peak in a s -wave superconductor, and a T^3 power law behavior in a d -wave superconductor. In the newly discovered high- T_C iron pnictide superconductors³⁻⁶, which are probably multiple-gap superconductors⁷⁻¹³, however, the temperature dependence of the ^{75}As SLRR below T_C varies dramatically with dopings. The SLRR of ^{75}As follows a power-law temperature dependence by $1/T_1 \sim T^n$, with the value of n varies from 6 to 1.5¹⁴⁻²⁵. It is unclear if the different value of n is caused by a change of the pairing symmetry with doping, a disorder scattering effect in an $S\pm$ gap superconductor²⁶⁻²⁸, or other unknown mechanism.

So far, NMR studies in iron pnictides were mostly performed on ^{75}As . From the Hebel-Slichter formulation, the NMR SLRR of all nuclei on the same material should have the same temperature dependence, regardless of s -wave or d -wave superconductivity. The underlying physics is that the SLRR is primarily determined by electron excitations, with the electron density of states (DOS) depending on the gap symmetry and the gap amplitude. In this letter, we present our NMR studies on high-quality $\text{NaFe}_{0.95}\text{Co}_{0.05}\text{As}$ superconductors. The NMR is performed on three nuclei, ^{23}Na , ^{75}As and ^{59}Co . Below T_C , the SLRR show a power-law like behavior on all sites, but with very different power-law exponent n on three nuclei. Our analysis indicates that such non-scale behavior is well understood by two superconducting gaps but with different gap sizes. We further found that the large gap on the cobalt site is much smaller compared with other sites. Since cobalt serves as a dopant, such

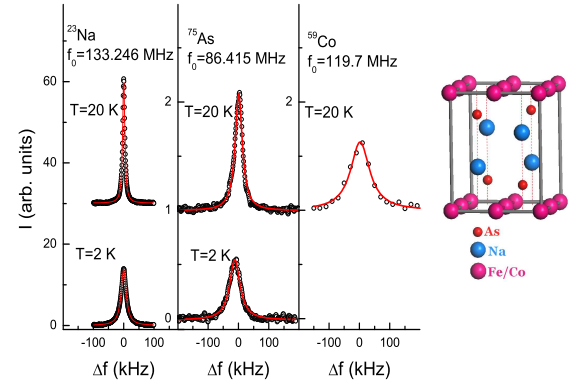


FIG. 1: (color online) Left panel: The NMR spectrum (dotted lines) of ^{23}Na , ^{75}As , and ^{59}Co of a $\text{NaFe}_{0.95}\text{Co}_{0.05}\text{As}$ single crystal at $T=20\text{ K}$ (above T_C) and $T=2\text{ K}$ (below T_C) with an applied field of 11.85 Tesla along the c -axis. The solid lines are the Lorentz function fitting. Right panel: A sketch of the $\text{NaFe}_{1-x}\text{Co}_x\text{As}$ unit cell.

spatial variation of the gap value suggests a local suppression of gap amplitude on the dopant site.

The growth of our electron-doped $\text{NaFe}_{0.95}\text{Co}_{0.05}\text{As}$ superconducting single crystals has been reported previously²⁹. The same sample is used here, and the superconducting transition is indicated by the sharp transition from the magnetization and resistivity at $T_C \approx 18\text{ K}$ ²⁹. Our NMR measurements were performed on ^{23}Na , ^{75}As , and ^{59}Co , with 6 Tesla and 11.85 Tesla magnetic field, and temperatures down to 1.5 K.

As shown in Fig. 1, Na, Co and As atoms reside on three typical positions in the lattice³⁰. Their typical NMR spectra are also shown in Fig. 1, and all lineshapes

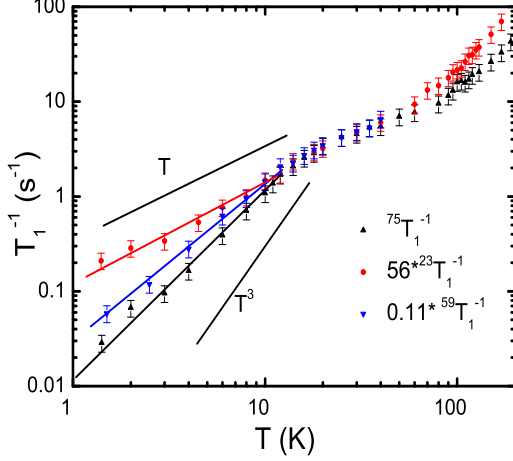


FIG. 2: (color online) The temperature dependent spin-lattice relaxation of ^{23}Na , ^{75}As and ^{59}Co of a $\text{NaFe}_{0.95}\text{Co}_{0.05}\text{As}$ single crystal under a 11.85 Tesla magnetic field along the c-axis.

are fit by Lorentz function. At $T = 20$ K, a temperature slightly above T_C , the full width of half maximum (FWHM) of the spectrum is about 8 kHz, 20 kHz and 34 kHz for ^{23}Na , ^{75}As and ^{59}Co , respectively. The narrow linewidth at such a low temperature and a high field indicates that the quality of our sample is very high. Below T_C , the spectrum is significantly broadened due to the distribution of magnetic fields around the vortex core³¹.

Our spin-lattice relaxation is measured by an inversion pulse method. The SLRR in a solid follows

$$1/T_1T = \frac{\pi k_B \gamma_n^2}{(\gamma_e \hbar)^2} \sum_q A_{hf}^2(q) \frac{\chi''_{\perp}(q, \omega)}{\omega}, \quad (1)$$

where $A_{hf}(q)$ is the hyperfine coupling constant, and $\chi''_{\perp}(q, \omega)$ is the imaginary part of the electronic dynamical susceptibility perpendicular to the magnetic field.

The SLRR of a $\text{NaFe}_{0.95}\text{Co}_{0.05}\text{As}$ single crystal under a 11.85 Tesla magnetic field is shown in Fig. 2. The 6 Tesla data (not shown in figure) gives identical results, showing no field-dependent behavior. The SLRR results show that the hyperfine coupling orders as $^{59}A_{hf} > ^{75}A_{hf} > ^{23}A_{hf}$. For comparison purpose, $1/^{23}T_1$ and $1/^{59}T_1$ are multiplied by a factor of 56 and 0.11, respectively. Above T_C , the SLRRs of three sites show similar temperature dependence. From 80 K to 200 K, $1/T_1T$ increases rapidly with temperature, and such behavior is known as a pseudogap-like phenomena reported in other iron pnictides³². Between 80 K and T_C , the SLRR of all sites is weakly temperature dependent, which is an indication of spin fluctuations³².

The Superconducting transition is shown by a drop of $1/T_1$ on all three sites. Similar to reports on other iron pnictides, no coherence peak is found in $\text{NaFe}_{0.95}\text{Co}_{0.05}\text{As}$, suggesting an unconven-

tional superconductor^{14–25}. Below T_C , $1/^{23}T_1$, $1/^{59}T_1$ and $1/^{75}T_1$ show power-law-like temperature dependence ($1/T_1 \approx T^n$), but the power law exponent are different with $n \approx 2$ for ^{75}As , $n \approx 1.7$ for ^{59}Co , and $n \approx 1.0$ for ^{23}Na . The sequential decrease of n suggests more contributions from the low energy excitations.

These SLRRs data cannot be fit by a single *s*-wave or a single *d*-wave function. Here we attempt to fit the data by a two-gap function, like in other iron arsenide superconductors²⁰. The spin-lattice relaxation for a two-gap Fermi liquid superconductor is approximated by,

$$1/T_{1n} = 2 \sum_{i=1,2} \int_0^{\infty} (A_{hf}^i N_0^i(E))^2 f(E)(1-f(E)) dE \quad (2)$$

$$T_{1n}/T_{1s} = \frac{2}{k_B T} \sum_{i=1,2} \int_0^{\infty} (d_S^i(E))^2 f(E)(1-f(E)) dE \quad (3)$$

where T_{1n} and T_{1s} are the spin-lattice relaxation time of the normal state and the superconducting state, respectively. N_0^i ($i=1,2$) is the normal state electron density of states (DOS) of each band, A_{hf}^i is the hyperfine coupling of the nucleus to each band, and $f(E)$ is the Fermi-Dirac distribution function with $f(E) = 1/(e^{-E/k_B T} + 1)$. Assuming a hyperbolic Fermi surface with N_0^1 and N_0^2 as constants, we define an *effective* normal state DOS $d_0^i \equiv A_{hf}^i N_0^i / D_0 \equiv A_{hf}^i N_0^i / (A_{hf}^1 N_0^1 + A_{hf}^2 N_0^2)$ with $d_0^1 + d_0^2 = 1$, and an *effective* superconducting state DOS $d_S^i(E) \equiv A_{hf}^i N_S^i(E) / D_0$ with N_S^i as the DOS in each superconducting band. Then d_S^i is simplified as $d_S^i \equiv d_0^i N_S^i / N_0^i$, with N_S^i / N_0^i as a functions of two superconducting gaps Δ_S^1 and Δ_S^2 , depending on the detailed gap symmetry. In the end, Eq. 2 and Eq. 3 contain only four fitting parameters, D_0 , d_0^1 , Δ_S^1 and Δ_S^2 .

Since the system has spin fluctuations, we first fit the normal state SLRR data by $1/T_1T \sim A/(T + \Theta)$ between T_C and 80 K. The $1/T_1$ data at all temperatures are then multiplied by $(T + \Theta)/\Theta$ to remove the spin fluctuation effect so that the Fermi liquid assumption in Eq. 2 holds. Finally, we fit the data by Eq. 2 (above T_C) and Eq. 3 (below T_C) with the same parameters.

TABLE I: The two-gap *d*-wave fitting parameters of the spin-lattice relaxation rate of ^{23}Na , ^{75}As , and ^{59}Co .

site	d_0^1	Δ_S^1 (meV)	Δ_S^2 (meV)
^{75}As	0.78	2.84 ± 0.15	0.26 ± 0.05
^{59}Co	0.68	1.81 ± 0.15	0.24 ± 0.05
^{23}Na	0.57	2.84 ± 0.15	0.20 ± 0.05

We first use a two-gap *d*-wave fitting, assuming the gap varies with angle by $\Delta_i(\phi) = \Delta_S^i \cos(2\phi)$. The effective DOS, by averaging out the angle dependence, is given by $d_S^i = d_0^i \frac{2}{\pi} K(\frac{\Delta_S^i}{E})$ for $E > \Delta_S^i$, and $d_S^i = d_0^i \frac{2}{\pi} \frac{E}{\Delta_S^i} K(\frac{E}{\Delta_S^i})$ for $E < \Delta_S^i$, where $K(x)$ is an elliptic function. A good fitting is obtained for the three nuclei as shown in Fig. 3(a), and the total effective DOS ($= d_S^1 + d_S^2$) below

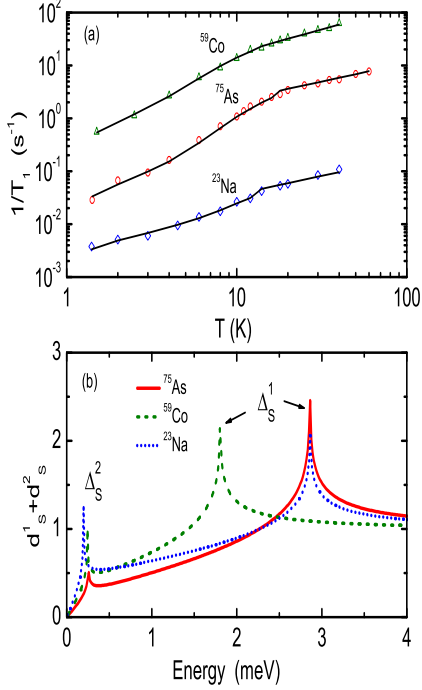


FIG. 3: (color online) (a) The low-temperature ^{23}Na , ^{75}As , and ^{59}Co spin-lattice relaxation rate (symbols) and the fittings (solid lines) by the two-gap d -wave symmetry as described in the text. (b) The effective electron density of states on ^{23}Na , ^{75}As , and ^{59}Co sites obtained from the fittings.

T_C are depicted in Fig. 3(b). The fitting parameters for each nucleus are listed in Table I. The close values of the large gap Δ_S^1 and the small gap Δ_S^2 among all nuclei suggest that our fittings are physically reasonable.

As shown in Fig. 3(b), the effective DOS is peaked at two energies corresponding to the gap value $E = \Delta_S^1$ and $E = \Delta_S^2$. The small gaps are similar for all sites with $2\Delta_S^2/k_B T_C \approx 0.3$. The large gap Δ_S^1 are similar on the As and the Na sites with $2\Delta_S^1/k_B T_C \approx 3.7$, but is much smaller on the Co site with $2\Delta_S^1/k_B T_C \approx 2.3$. The smaller Δ_S^1 on the cobalt site suggests a spatial suppression of gap close to it. Since Co serves as a dopant in the lattice, the gap suppression is probably caused by a local scattering effect from doping. Similarly, a local gap suppression by dopant has been reported by STM studies in the cuprates³³.

In Table I, a systematic decrease of d_0^1 ($E = \Delta_S^1$) is seen in the order of ^{75}As , ^{59}Co , and ^{23}Na , which is reversely demonstrated by the increase of the effective DOS close to small gap position ($E = \Delta_S^2$) in Fig. 3(b). Physically, it suggests that the ^{23}Na senses more low energy excitations than other sites, which explains the smaller power law exponent n of the SLRR on ^{23}Na . With d_0^1 rewritten as $d_0^1 \equiv 1/(1 + (A_{hf}^2/A_{hf}^1)(N_0^2/N_0^1))$, d_0^1 is determined by the ratios of the actual DOS in two bands N_0^1/N_0^2 and the ratio of the hyperfine coupling to two

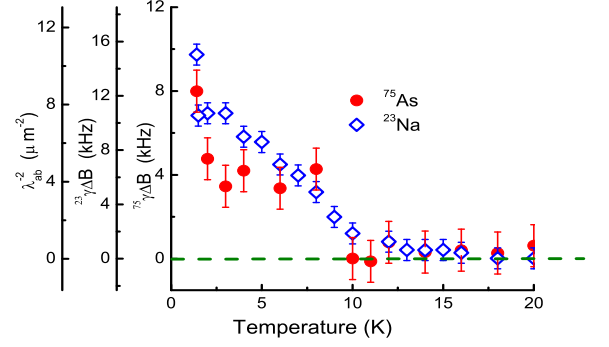


FIG. 4: (color online) The increase of the NMR linewidth of ^{23}Na and ^{75}As spectrum below T_C . Both linewidth are scaled to λ_{ab}^{-2} as shown by the vertical axis (see text), where λ_{ab} is the penetration depth.

bands A_{hf}^1/A_{hf}^2 . It is reasonable to assume that N_0^1/N_0^2 does not vary with nucleus sites, and is determined by the two electron bands. A_{hf}^1/A_{hf}^2 , however, could vary with nucleus site, since the hyperfine coupling is momentum dependent (see Eq. 1), and the Fermi surfaces of different bands of the iron arsenides are separated in the Brillouin zone³⁴. Then the final conclusion is reached that the smaller power-law exponent n of the SLRR is caused by a stronger local hyperfine coupling of the nucleus to the band with the small gap.

Before going further, we confirm that our SLRR for all nuclei are intrinsic for several reasons. First, the spin recovery for each nucleus has only one T_1 component below T_C . Second, the normal state $1/T_1$ on all sites shows a similar temperature dependence, which is consistent with other electron-doped iron arsenide³². Finally and most importantly, we confirmed that ^{23}Na and ^{59}Co signals are excited from the same region around the vortex core within the penetration depth. The penetration depth is evaluated from the spectrum broadening below T_C due to the local distribution of fields around a vortex core³¹. For each nucleus, the penetration depth λ_{ab} is calculated by $\Delta B = \Delta f/\gamma_n \approx 0.0609\phi_0/\lambda_{ab}^2$ below T_C ³¹, where ϕ_0 is the quantum flux, Δf is the linewidth, and γ_n is the gyromagnetic factor of the nucleus. As shown in Fig. 4, the penetration depth approaches $\lambda_{ab} \approx 0.3 \mu\text{m}$ as $T \rightarrow 0$ K from both ^{23}Na and ^{75}As measurements. Such penetration depth is typical for iron arsenide with a similar T_C ³⁵.

Therefore, our analysis suggests that the temperature dependence of the NMR SLRR below T_C is affected by two effects. First, the gap is locally suppressed by the disorder effect on the dopant site. Second, the different power-law exponent n of the SLRR on each nucleus is well understood in a superconductor with a large gap and a small gap. It is worthwhile to mention that ARPES may not be able to resolve the small gap. Although our fitting scheme is based on a d -wave symmetry, the conclusion is also valid on a two-gap superconductor with other sym-

metries. For example, we believe an anisotropic two-gap s -wave fitting should also work, if a similar electron DOS is obtained as that of the d -wave fitting. The proposed s_{\pm} gap symmetry with strong scatterings^{26,27,36} may also work.

Our conclusion that the power-law behavior of the SLRR varies with local hyperfine couplings and local gap amplitude may shed light on ^{57}As NMR studies on other iron pnictides in two aspects. First, the local gap suppression from the dopant should be stronger with the increase of the doping. As a result, doping may cause more low energy excitations, and lower the power-law exponent as shown on the cobalt site. Second, with the increase of doping, the local hyperfine couplings $A_{hf}(q)$ of ^{57}As on the Fermi surface may also vary with doping, because the Fermi surface changes dramatically with doping in iron arsenides³⁷. In both cases, the change of the power-law exponent n are not necessarily related to the change of the gap symmetry.

In summary, our NMR study on $\text{NaFe}_{0.95}\text{Co}_{0.05}\text{As}$ single crystals shows that the SLRR on ^{23}Na , ^{59}Co , and ^{75}As sites has very different temperature dependent power-law behavior below T_C . Our analysis suggests that such non-scale behavior is well described by the Hebel-Slichter formulation based on a two-gap superconductor with a large gap and a very small gap, regardless of the detailed gap symmetry. We also found that the large gap on the Co-dopant site is strongly suppressed, probably due to the disorder effect. To our knowledge, this is the first report of a local gap suppression on the dopant site, and the effect may be verified by scanning probes such as STM.

The Authors acknowledge Dr. Wei Bao, Qiang Han, Zhongyi Lu, Tiesong Zhao for helpful discussions. W.Y. and G.F.C are supported by the National Basic Research Program of China. W.Y. is also supported by Program for New Century Excellent Talents in University.

-
- * Electronic address: wgyu'phy@ruc.edu.cn
- ¹ L. C. Hebel and C. P. Slichter, Phys. Rev. **113**, 1504 (1959).
 - ² L. C. Hebel, Phys. Rev **116**, 79 (1959).
 - ³ Y. Kamihara, T. Watanabe, M. Hirano, and H. Hosono, J. Am. Chem. Soc. **130**, 3296 (2008).
 - ⁴ X. H. Chen, T. Wu, G. Wu, R. H. Liu, H. Chen, and D. F. Fang, Nature **453**, 761 (2008).
 - ⁵ G. F. Chen, Z. Li, D. Wu, G. Li, W. Z. Hu, J. Dong, P. Zheng, J. L. Luo, and N. L. Wang, Phys. Rev. Lett. **100**, 247002 (2008).
 - ⁶ Z. A. Ren et al., Mater. Res. Inno. **12**, 105 (2008).
 - ⁷ I. I. Mazin, D. J. Singh, M. D. Johannes, and M. H. Du, Phys. Rev. Lett. **101**, 057003 (2008).
 - ⁸ V. Cvetkovic and Z. Tesanovic, Europhysics Lett. **85**, 37002 (2009).
 - ⁹ K. Seo, B. A. Bernevig, and J. Hu, Phys. Rev. Lett. **101**, 206404 (2008).
 - ¹⁰ K. Kuroki, S. Onari, R. Arita, H. Usui, Y. Tanaka, H. Kontani, and H. Aoki, Phys. Rev. Lett. **101**, 087004 (2008).
 - ¹¹ F. Wang, H. Zhai, Y. Ran, A. Vishwanath, and D. Lee, Phys. Rev. Lett. **102**, 047005 (2009).
 - ¹² K. Nakayama, T. Sato, P. Richard, Y.-M. Xu, Y. Sekiba, S. Souma, G. F. Chen, J. L. Luo, N. L. Wang, H. Ding, et al., EPL **85**, 67002 (2009).
 - ¹³ H. Ding, P. Richard, K. Nakayama, K. Sugawara, T. Arakane, Y. Sekiba, A. Takayama, S. Souma, T. Sato, T. Takahashi, et al., EPL **83**, 47001 (2008).
 - ¹⁴ H.-S. Lee, M. Bartkowiak, J.-H. Park, J.-Y. Lee, J.-Y. Kim, N.-H. Sung, B. K. Cho, C.-U. Jung, J. S. Kim, and H.-J. Lee, Phys. Rev. B **80**, 144512 (2008).
 - ¹⁵ H.-J. Grafe, D. Paar, G. Lang, N. J. Curro, G. Behr, J. Werner, J. Hamann-Borrero, C. Hess, N. Leps, R. Klingeler, et al., Phys. Rev. Lett. **101**, 047003 (2008).
 - ¹⁶ Y. Kobayashi et al., J. Phys. Soc. Jpn. **78**, 073704 (2009).
 - ¹⁷ H. Mukuda et al., J. Phys. Soc. Jpn. **77**, 093704 (2008).
 - ¹⁸ N. Terasaki et al., J. Phys. Soc. Jpn. **78**, 013701 (2009).
 - ¹⁹ H. Fukazawa, T. Yamazaki, K. Kondo, Y. Kohori, N. Takeshita, P. M. Shirage, K. Kihou, K. Miyazawa, H. Kito, H. Eisaki, et al., J. Phys. Soc. Jpn. **78**, 033704 (2009).
 - ²⁰ K. Matano, Z. A. Ren, X. L. Dong, L. L. Sun, Z. X. Zhao, and G. Q. Zheng, EPL **83**, 57001 (2008).
 - ²¹ S. Kawasaki, K. Shimada, G. F. Chen, J. L. Luo, N. L. Wang, and G. qing Zheng, Phys. Rev. B **78**, 220506 (R) (2008).
 - ²² K. Matano, G. L. Sun, D. L. Sun, C. T. Lin, and G. Q. Zheng, Europhys. Lett. **87**, 27012 (2009).
 - ²³ F. Hammerath, S.-L. Drechsler, H.-J. Grafe, G. Lang, G. Fuchs, G. Behr, I. Eremin, M. M. Korshunov, and B. Büchner, Cond-Mat/0912.3682v1 (2009).
 - ²⁴ Y. Nakai, T. Iye, S. Kitagawa, K. Ishida, S. Kasahara, T. Shibauchi, Y. Matsuda, and T. Terashima, Cond-mat/0908.0625v2 (2009).
 - ²⁵ S. W. Zhang, L. Ma, Y. D. Hou, J. Zhang, T.-L. Xia, G. F. Chen, J. P. Hu, G. M. Luke, and W. Yu, Phys. Rev. B **81**, 012503 (2010).
 - ²⁶ Y. Bang, H.-Y. Choi, and H. Won, Phys. Rev. B **79**, 054529 (2009).
 - ²⁷ K. Seo, C. Fang, B. A. Bernevig, and J. Hu, Phys. Rev. B **79**, 235207 (2009).
 - ²⁸ A. V. Chubukov, M. G. Vavilov, and A. B. Vorontsov, Phys. Rev. B **80**, 140515 (R) (2009).
 - ²⁹ T.-L. Xia, J. B. He, D. M. Wang, and G. F. Chen, Cond-mat/1001.3311 (2010), (unpublished).
 - ³⁰ S. Li, C. de la Cruz, Q. Huang, G. F. Chen, T.-L. Xia, J. L. Luo, N. L. Wang, and P. Dai, Phys. Rev. B **80**, 020504 (R) (2009).
 - ³¹ E. H. Brandt, Phys. Rev. B **37**, 2349 (1988).
 - ³² F. L. Ning, K. Ahilan, T. Imai, A. S. Sefat, M. A. McGuire, B. C. Sales, D. Mandrus, P. Cheng, B. Shen, and H.-H. Wen, Phys. Rev. Lett. **104**, 037001 (2010).
 - ³³ T. S. Nunner, B. M. Andersen, A. Melikyan, and P. J. Hirschfeld, Phys. Rev. Lett. **95**, 177003 (2005).
 - ³⁴ D. J. Singh, Phys. Rev. B **78**, 094511 (2008).
 - ³⁵ J. P. Carlo et al., Phys. Rev. Lett. **102**, 087001 (2009).
 - ³⁶ A. V. Chubukov, D. V. Efremov, and I. Eremin, Phys. Rev.

B **78**, 134512 (2008).

³⁷ T. Sato et al., Phys. Rev. Lett. **103**, 047002 (2009).